

A Surface Impedance Approach for Modeling Transmission Line Losses in FDTD

Werner Thiel

Abstract—This letter presents a concept for an ultrawide-band modeling of transmission line losses in the three-dimensional (3-D) finite-difference time-domain (FDTD) scheme. The approach makes use of the surface impedance boundary condition (SIBC) employing a two-port model for a lossy conducting layer with some modifications at the edges of the metal lines. Using this model, the frequency-dependent inner inductance as well as the resistive losses are included up to very high frequencies. Furthermore, the thickness of the metallization can also be extended over several cells, and the real current distribution on the surface can be considered. For validation, the attenuation coefficient and the effective permittivity of a coplanar line are compared to results achieved from the mode-matching technique.

Index Terms—FDTD methods, losses, skin effect.

I. INTRODUCTION

LOSSES in microwave circuits play an important role in the prediction of the electromagnetic behavior, but can be taken into account only partially in the finite-difference time-domain (FDTD) method. In the literature, several partial solutions to this problem have been proposed [1]–[3]. These approaches are limited in the frequency range or in the thickness of the metallization.

This contribution presents an ultrawide-band approximation of metallic losses using the SIBC approach based on a two-port model for the surfaces and a simplified model for the edges as described in Sections II and III. This model enables an adjustment of the numerical accuracy, and transmission lines covering several cells in thickness can be considered. Furthermore, different current densities at the top and bottom side of the metallization are considered.

II. TWO-PORT MODEL FOR A LOSSY CONDUCTING LAYER

Fig. 1 shows a lossy conducting layer bounded by two regular surfaces S_1 and S_2 . The layer is characterized by the thickness d , the permittivity ϵ , the permeability μ , and the conductivity σ . Assuming the surfaces are plane and the conductivity σ is much greater than $\omega\epsilon$, a TEM-approximation for the electromagnetic field can be formulated. The relationship between the tangential electric and magnetic field components infinitely closed to the surfaces S_1 and S_2 is given by the following [4]:

$$\begin{pmatrix} E_1 \\ E_2 \end{pmatrix} = \begin{pmatrix} Z_{11} & Z_{12} \\ Z_{21} & Z_{22} \end{pmatrix} \begin{pmatrix} H_1 \\ H_2 \end{pmatrix} \quad (1)$$

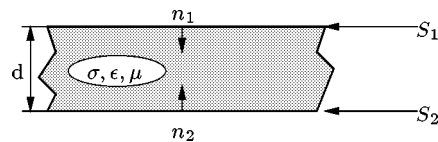


Fig. 1. Layer of lossy conductor.

where

$$Z_{11} = Z_{22} = \sqrt{\frac{j\omega\mu}{\sigma}} \coth \sqrt{j\omega\mu\sigma d^2} \quad (2)$$

and

$$Z_{12} = Z_{21} = \sqrt{\frac{j\omega\mu}{\sigma}} / \sinh \sqrt{j\omega\mu\sigma d^2}. \quad (3)$$

To facilitate a subsequent transformation in the time domain, the two-port model is written in the slightly different form

$$E = \frac{1}{j\omega} \mathbf{Z}(j\omega H) \quad \text{with} \quad \hat{\mathbf{Z}} = \frac{1}{j\omega} \mathbf{Z}. \quad (4)$$

Inverse Fourier transformation yields the corresponding time domain convolution of

$$E(t) = \hat{\mathbf{Z}}(t) * \frac{\partial}{\partial t} H(t) \quad (5)$$

where $\hat{\mathbf{Z}}(t)$ is the equivalent surface-impedance impulse response by inverse Laplace transformation

$$\hat{Z}_{11}(t) = \hat{Z}_{22}(t) = \frac{1}{\sigma d} \left(1 + 2 \sum_{n=1}^{\infty} \exp\left(-\frac{n^2 \pi^2}{\mu \sigma d^2} t\right) \right) \quad (6)$$

$$\begin{aligned} \hat{Z}_{12}(t) &= \hat{Z}_{21}(t) \\ &= \frac{1}{\sigma d} \left(1 + 2 \sum_{n=1}^{\infty} (-1)^n \exp\left(-\frac{n^2 \pi^2}{\mu \sigma d^2} t\right) \right). \quad (7) \end{aligned}$$

Applying the surface impedance boundary condition (1) on the Yee's mesh and taking the field components closest to the surfaces as shown in Fig. 2, the electric field components can be expressed by the time derivation of the magnetic field

$$\pm E_{y,z}^{(1)} \Big|_n = -\hat{Z}_{11} * \frac{\partial}{\partial t} H_{z,y}^{(1)} \Big|_n + \hat{Z}_{12} * \frac{\partial}{\partial t} H_{z,y}^{(2)} \Big|_n \quad (8)$$

$$\pm E_{y,z}^{(2)} \Big|_n = -\hat{Z}_{21} * \frac{\partial}{\partial t} H_{z,y}^{(1)} \Big|_n + \hat{Z}_{22} * \frac{\partial}{\partial t} H_{z,y}^{(2)} \Big|_n. \quad (9)$$

Together with Faraday equations

$$-\frac{\partial}{\partial t} H_{y,z}^{(2)} \Big|_n \mu = \nabla \times E^{(2)} \Big|_{y,z} \quad (11)$$

Manuscript received October 20, 1999; revised February 1, 2000.
The author is with the Department of Microwave Techniques, University of Ulm, 89069 Ulm, Germany.
Publisher Item Identifier S 1051-8207(00)03351-1.

the system of (8)–(11) can be solved for the tangential magnetic field components, leading to a boundary condition for the magnetic field. In this case, the convolution integrals $\hat{Z}_{ij} * (\partial/\partial t)H_{z,y}^{(j)}$ are approximated by $\sum_{m=0}^n \hat{Z}_{ij}(m\Delta t)(\partial/\partial t)H_{z,y}^{(j)}|^m \Delta t$ assuming the fields piecewise constant in time and applying the midpoint rule for the integration. This full-sum convolution needs the complete history of the fields resulting in increasing memory requirements and simulation time after each time step. As the time response of the surface impedance is a sum of exponential functions, a recursive implementation is possible. The infinite sum of exponentials in the time domain has to be reduced to a finite number of terms. As a consequence, this approximation of the impedance leads to a frequency-dependent error. Fig. 3 shows the relative error of Z_{11} , $\epsilon = |Z_{11}^{\text{app}}(\omega) - Z_{11}(\omega)|/|Z_{11}(\omega)|$, in the frequency domain for different number of summation terms as a function of the normalized frequency f/f_g . The skin depth is half the thickness of the conducting layer. A relative error of less than 10% for Z_{11} can be achieved by using 40 terms, whereas the simulations of transmission line losses show that this number of terms may be reduced without an essentially decrease of accuracy. The accuracy of Z_{12} has the same order and shows a similar behavior.

III. SIMPLIFIED MODEL FOR EDGES

In this section, a reduced model for the surface impedance is presented which leads to less computational effort and increasing accuracy using the same number of summation terms. This model is also suited for the treatment of edges where the two-port model cannot be employed. If the electric field on the top and bottom side of a metallization has the same value, the two-port model can be simplified to

$$\begin{pmatrix} E_1 \\ E_2 \end{pmatrix} = \begin{pmatrix} Z_{11}(d/2) & 0 \\ 0 & Z_{22}(d/2) \end{pmatrix} \begin{pmatrix} H_1 \\ H_2 \end{pmatrix}. \quad (12)$$

This leads to an uncoupled scheme easier to handle for the edges. Due to the factor 0.5 in the argument, equivalent to a halved thickness, less terms are required for the same accuracy, because the normalized frequency now is four times higher than in the two-port model. Employing this approximation, the boundary values of the surface impedance for low and high frequencies are exactly the same as for the complete two-port model. Only in the frequency range, where the skin depth is twice the thickness of the metal layer, small deviations may occur.

IV. MODIFICATION OF THE MODEL

At the edges of a transmission line, the two-port model cannot be used for the surface impedance because there is no counterpart for the H -fields at the abutting face of the line. Two cases of edges have to be considered. First, a formulation is given when the thickness of the layer is smaller than the cell size. In the second case, the layer covers more than one cell. Fig. 4 shows the cross section of an edge of a thin transmission line together with three magnetic field components, each to be modeled separately. The aim of the algorithm is to provide the correct edge impedance for both dc and the high-frequency cases. For higher

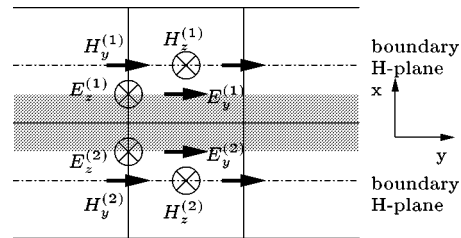


Fig. 2. Layer of lossy conductor in the Yee mesh.

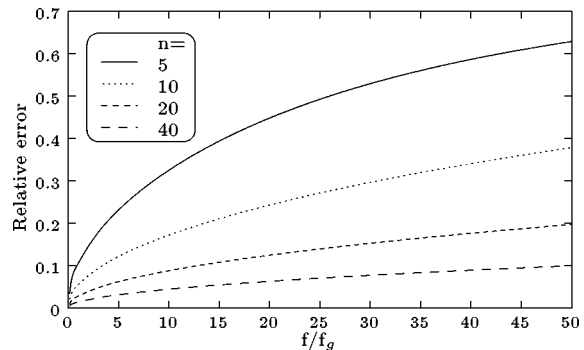


Fig. 3. Relative error of Z_{11} with different numbers of exponentials; frequency is normalized to $f_g = 4/(\pi\mu\sigma d^2)$.

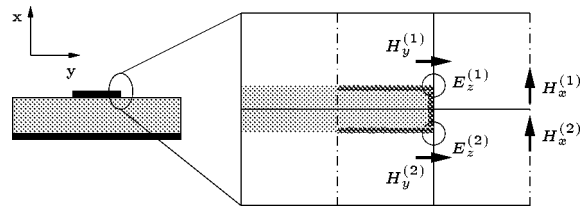


Fig. 4. Cross section of an edge in the Yee mesh; cell size is larger than the conducting layer; propagation of the wave in z -direction.

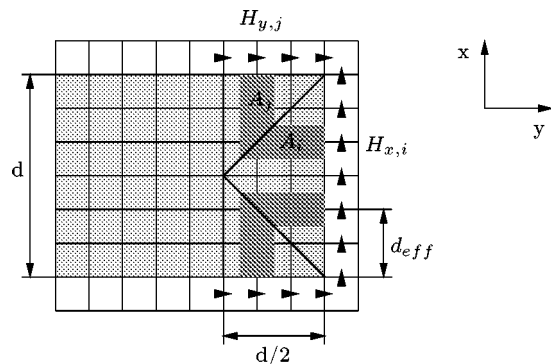


Fig. 5. Cross section of an edge in the Yee mesh; conducting layer is several cells high; propagation of the wave in z -direction.

frequencies, the current concentrates on the surface of the transmission line as marked in Fig. 4. The current in the abutting face yielding a lower impedance has to be included in the effective surface impedance of the edge. The resulting effective length for the impedance for both edges is $l_{\text{eff}} = \Delta y/2 + d/2$. For the dc case, the surface impedance has to represent the dc resistance related to the cross section of the corner. This leads to an effective thickness of the edge $d_{\text{eff}} = \Delta y d / (4l_{\text{eff}})$. To consider different current densities on the top and the bottom side of the line, the

electric and magnetic fields at the edge are split into two parts. The relationship between the electric and magnetic fields at the edge results in

$$E_z^{(1)} = \left(\frac{\partial}{\partial t} H_y^{(1)} \frac{\Delta y}{2} - \frac{\partial}{\partial t} H_x^{(1)} \frac{\Delta x}{2} \right) \hat{Z}_{11}(d_{\text{eff}}) \frac{1}{l_{\text{eff}}} \quad (13)$$

$$E_z^{(2)} = \left(-\frac{\partial}{\partial t} H_y^{(2)} \frac{\Delta y}{2} - \frac{\partial}{\partial t} H_x^{(2)} \frac{\Delta x}{2} \right) \hat{Z}_{11}(d_{\text{eff}}) \frac{1}{l_{\text{eff}}}. \quad (14)$$

Together with the Faraday equations for $H_y^{(1)}, H_y^{(2)}, H_x^{(1)}, H_x^{(2)}$, and the H_x field ($H_x = (H_x^{(1)} + H_x^{(2)})/2$), the system can be solved for the three unknown magnetic field components. This approach can also be applied for a layer with a height of one cell. If the conducting sheet covers more than one cell, as shown in Fig. 5, the method has to be modified. The surface impedance in the edge region is modified in the same way as in the previous case. All affected H -field components are computed with the reduced two-port model. Here, the effective length of each cell of the surface is the cell size itself, except at the corner, where the impedances have to be doubled. With respect to a correct dc modeling, effective thicknesses $d_{\text{eff}}^{x,i} = A_i^x / \Delta x_i$ and $d_{\text{eff}}^{y,j} = A_j^y / \Delta y_j$ have to be introduced for the surface impedance Z_{11} at the edge. This approach leads to the real dc impedance of $2/(\sigma d^2)$ and to a homogenous skin depth at the edge for higher frequencies.

V. VALIDATION AND RESULTS

For empirical validation, a coplanar line has been simulated. The coplanar line on an InP substrate has a center conductor width of $20 \mu\text{m}$ and a ground-to-ground spacing of $54 \mu\text{m}$. The gold metallization is $3 \mu\text{m}$ thick, and the skin depth is $1.5 \mu\text{m}$ at 2.7 GHz . The center conductor is discretized by seven cells in the y -direction and one cell in height. The simulation results using 30 exponentials are compared to mode-matching data according to [5]. In Figs. 6 and 7, the attenuation and the effective permittivity of the coplanar line are shown. There is a good agreement between the FDTD and the mode-matching results in a wide-frequency band.

VI. CONCLUSION

An efficient method for including transmission line losses in the FDTD scheme is presented. In contrast to other approaches, this abstract modeling based on a modified surface impedance boundary condition can be applied to many problems with minor limitations. To this end, there are no restrictions concerning the frequency range and the size of the metal strip and the extension of the thickness over several cells. As the

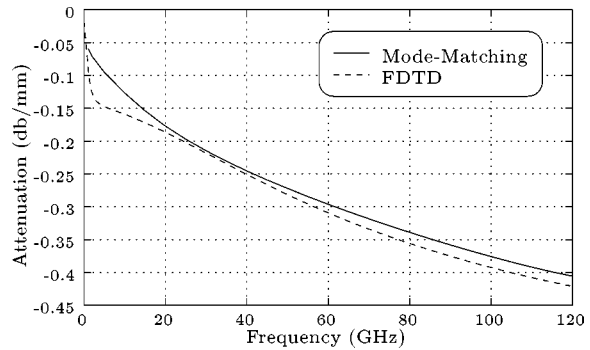


Fig. 6. Attenuation of the coplanar line on InP substrate; $d = 20 \mu\text{m}$; $g = 54 \mu\text{m}$; $t = 3 \mu\text{m}$ (gold).

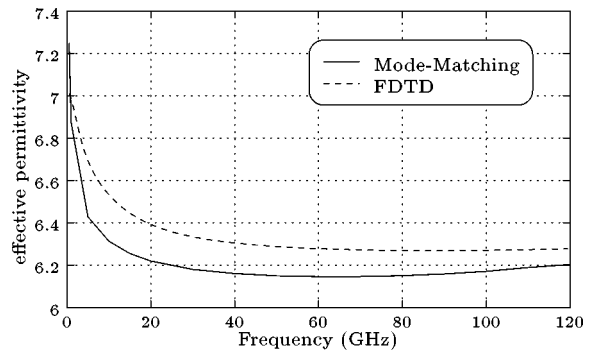


Fig. 7. Effective permittivity of the coplanar line on InP substrate; $d = 20 \mu\text{m}$; $g = 54 \mu\text{m}$; $t = 3 \mu\text{m}$ (gold).

impedance in the time domain can be written in a sum of exponentials resulting in recursive implementation, the time requirement for calculating the metal line is lower than the FDTD calculation of the remaining structure. Finally, the simulation results are validated by the mode-matching method results over a wide frequency range.

REFERENCES

- [1] J. Beggs *et al.*, "Finite difference time domain implementation of surface impedance boundary conditions," *IEEE Trans. Antennas Propagat.*, vol. 40, pp. 49–56, Jan. 1992.
- [2] L.-K. Wu and L.-T. Han, "Implementation and application of resistive sheet boundary condition in the finite difference time domain method," *IEEE Trans. Antennas Propagat.*, vol. 40, pp. 628–633, June 1992.
- [3] A. Lauer and I. Wolff, "A conducting sheet model for efficient wide band FDTD analysis of planar waveguides and circuits," in *IEEE MTT-S Int. Microwave Symp. Dig.*, 1999, pp. 1589–1592.
- [4] F. Bouzidi, H. Aubert, D. Bajon, and H. Boudrand, "Equivalent network representation of boundary conditions involving generalized trial quantities—Application to lossy transmission lines with finite metallization thickness," *IEEE Trans. Microwave Theory Tech.*, vol. 45, pp. 869–876, June 1997.
- [5] R. Schmidt and P. Russer, "Modeling of cascaded coplanar discontinuities by the mode-matching approach," *IEEE Trans. Microwave Theory Tech.*, vol. 43, pp. 2910–2917, Dec. 1995.